JOURNAL OF GUIDANCE, CONTROL, AND DYNAMICS
Vol. 18, No. 6, November–December 1995

Optimal Planar Interception with Terminal Constraints

Moshe Idan*
Technion—Israel Institute of Technology, Haifa 32000, Israel
Oded M. Golan†
RAFAEL, Ministry of Defense, Haifa 31021, Israel
and
Moshe Guelman‡
Technion—Israel Institute of Technology, Haifa 32000, Israel

In this paper, planar interception laws for maneuvering targets with known trajectories are presented. Optimal interception problems are defined, which include constraints on the initial and final flight-path angles of the interceptor. For cases where the initial flight-path angle can be freely assigned, it is included in the optimization problem. Analytical solutions for the planar interception problems are derived. Numerical examples that demonstrate the optimal trajectories are presented showing also the effect of the interceptor initial flight-path angle on the interception characteristics. It is shown that when the interceptor initial conditions can be optimized superior performance is obtained.

I. Introduction

EXTENSIVE work has been done on guidance laws for intercepting maneuvering targets. The classical proportional navigation law gives best results against nonmaneuvering targets.[1,2] In other cases, such as accelerating targets, proportional navigation may give poor performance. Linear optimal control theory was used to derive guidance laws that better treat maneuvering targets.[3,4] This approach is adequate for the terminal guidance phase, where the interceptor and target are moving close to collision course.

Singular perturbation theory was used to find approximate solutions for the nonlinear guidance problem.[5–7] The method separates slow and fast dynamics, resulting in low-order suboptimal solutions.

An optimal solution to the guidance problem for a maneuvering target, using exact nonlinear equations of motion in relative polar coordinates, was derived in Ref. 8. The work assumed constant interceptor speed, fixed initial and free final interceptor flight directions, perfect knowledge of the maneuvering target behavior, and a cost function that combines interception time and maneuvering energy expenditure. In Ref. 9, minimum-time trajectories used as time-to-go algorithms for a missile controlled by a linear quadratic guidance law were developed and the same guidance problem but for a nonmaneuvering target was considered. Using relative cartesian coordinates for the equations of motion, results were obtained for the fixed initial and free final interceptor flight-path directions.

The previously obtained analytical solutions can be applied to problems where the target behavior can be predicted or when continuous update of the guidance parameters, based on the updated target model, can be implemented. A typical example is the intercept of a ballistic missile in the boost phase, in which the target model can be estimated and its future behavior is predictable. Another example is midcourse guidance for long-range air-to-air missiles. The purpose of the midcourse guidance in this case is to bring the missile in an energy-efficient way to within a close distance from the target, where a terminal guidance phase starts.

In some cases the final approach direction may have preferred values for which higher hit probabilities are obtained. In Ref. 10, the interception problem of nonmaneuvering targets with terminal constraints is presented; however, the assumption that the target velocity and flight-path angle are constant is imbeded into the solution and thus cannot be extended to the maneuvering target case. Furthermore, if the interceptor can be launched in any direction, its initial flight direction can be optimally chosen.

The purpose of this paper is to find the optimal planar interception laws for maneuvering targets with a given final interception direction for either a given or a free initial interceptor flight direction. The case of a free final interception direction, considered previously in Refs. 8 and 9, will appear as a particular case of this more general solution.

In the next section the interception problem treated in this paper is presented. The solution to this problem is then derived in Sec. III, and some special interception scenarios are treated in Sec. IV. Numerical examples that demonstrate the trajectories obtained by the optimal solutions are presented in Sec. V, followed by conclusions. The Appendix presents the detailed solutions to the planar interception problems.

II. Problem Statement

The geometry used to define the interception problem presented in this paper is shown in Fig. 1. The interceptor I is moving at a constant speed V_I and can change its flight direction by applying bounded normal acceleration $|u| \leq U$. The target T is moving along an a priori known trajectory with known velocity $V_T(t)$. The coordinates (X_I, Y_I) and (X_T, Y_T) describe the location of the interceptor and the target, respectively, relative to the origin of an arbitrary reference coordinate system.

The interceptor equations of motion are

$$\dot{X}_I = V_I \cos\gamma_I, \qquad X_I(0) = X_{I_0} \tag{1}$$

$$\dot{Y}_I = V_I \sin\gamma_I, \qquad Y_I(0) = Y_{I_0} \tag{2}$$

$$\dot{\gamma}_I = \frac{u}{V_I} \tag{3}$$

Interception is defined by

$$X_I(t_f) = X_T(t_f) \tag{4}$$

$$Y_I(t_f) = Y_T(t_f) \tag{5}$$

In addition, the final interception geometry is specified by defining the final approach angle, i.e., the final flight-path angles of the interceptor and the target are related by

$$\cos[\gamma_I(t_f) - \gamma_T(t_f)] = \cos\Gamma_f \tag{6}$$

Received May 7, 1994; revision received March 27, 1995; accepted for publication April 7, 1995.

*Annie and Charles Corrin Academic Lecturer, Department of Aerospace Engineering. Member AIAA.
†Research Engineer. Member AIAA.
‡Professor, Department of Aerospace Engineering.

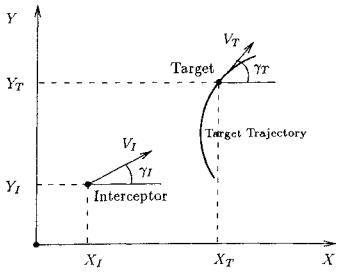

Fig. 1 Interception geometry.

where Γ_f is the required final approach angle. For example, $\Gamma_f = \pi$ represents a head-on interception. The cosine in Eq. (6) introduces the symmetry around the head-on direction and solves the 2π angle ambiguity. Since the target trajectory is assumed to be known, $X_T(t_f)$, $Y_T(t_f)$, and $\gamma_T(t_f)$ in Eqs. (4–6) are known functions of time.

The problem is to find $u(t)$, the control input time history, so that Eqs. (1–6) are satisfied and the performance index J, defined by

$$J = kt_f + \frac{1}{2}\int_0^{t_f} u^2(t)\,dt \tag{7}$$

is minimized while intercepting a target with a known trajectory.

In the above formulation, the normal acceleration of the interceptor is not constrained but is limited to realistic values by the second term of the performance index J and is controlled by the size of the weighting factor k. In general, larger k cause larger $|u(t)|$. For aerodynamically controlled interceptors, this term can also be interpreted as the energy required to overcome induced drag.

III. Optimal Planar Interception Solution

To construct the optimal solution, an additional variable χ is defined as

$$\dot{\chi} = k + \tfrac{1}{2}u^2, \qquad \chi(0) = 0 \tag{8}$$

Then the performance index of Eq. (7) becomes

$$J = \chi(t_f) \tag{9}$$

The optimization problem is solved by the maximum principle.[2] The Hamiltonian $\mathcal{H}$ for the system defined by Eqs. (1–3), (8), and (9) is

$$\mathcal{H} = \lambda_X V_I \cos\gamma_I + \lambda_Y V_I \sin\gamma_I + \lambda_\gamma \frac{u}{V_I} + \lambda_\chi\left(k + \frac{1}{2}u^2\right) \tag{10}$$

where λ_X, λ_Y, λ_γ, and λ_χ are the adjoint variables. The Hamiltonian is constant since it is not an explicit function of time. The necessary conditions for an optimal solution are

$$\dot{\lambda}_X = 0 \tag{11}$$

$$\dot{\lambda}_Y = 0 \tag{12}$$

$$\dot{\lambda}_\gamma = \lambda_X V_I \sin\gamma_I - \lambda_Y V_I \cos\gamma_I \tag{13}$$

$$\dot{\lambda}_\chi = 0 \tag{14}$$

$$\mathcal{H}_u = \lambda_\gamma / V_I + \lambda_\chi u = 0 \tag{15}$$

i.e., λ_X, λ_Y, and λ_χ are constant along the optimal trajectory. The boundary conditions of the adjoint variables are determined by the transversality conditions and depend on the state boundary conditions. For that, the endpoint function for the minimization problem is defined by the performance index of Eq. (9) and the boundary conditions of Eqs. (4–6) as

$$\Phi \triangleq -\chi_f + \nu_X\left(X_{I_f} - X_{T_f}\right) + \nu_Y\left(Y_{I_f} - Y_{T_f}\right) + \nu_\gamma\left[\cos\left(\gamma_{I_f} - \gamma_{T_f}\right) - \cos\Gamma_f\right] \tag{16}$$

where ν_X, ν_Y, and ν_γ are unknown constants. The transversality conditions are

$$\lambda_\chi(t_f) = \Phi_{\chi_f} = -1 \tag{17}$$

$$\lambda_X(t_f) = \Phi_{X_{I_f}} = \nu_X \tag{18}$$

$$\lambda_Y(t_f) = \Phi_{Y_{I_f}} = \nu_Y \tag{19}$$

$$\lambda_\gamma(t_f) = \Phi_{\gamma_{I_f}} = -\nu_\gamma \sin\left(\gamma_{I_f} - \gamma_{T_f}\right) \tag{20}$$

and

$$\mathcal{H}(t_f) = -\Phi_{t_f} = \nu_X \frac{\partial X_{T_f}}{\partial t_f} + \nu_Y \frac{\partial Y_{T_f}}{\partial t_f} - \nu_\gamma \sin\left(\gamma_{I_f} - \gamma_{T_f}\right)\frac{\partial \gamma_{T_f}}{\partial t_f} \tag{21}$$

Using Eqs. (18–20) in the last equation leads to

$$\mathcal{H}_f = \lambda_X V_{T_f} \cos\gamma_{T_f} + \lambda_Y V_{T_f} \sin\gamma_{T_f} + \lambda_{\gamma_f}\omega_{T_f} \tag{22}$$

where, from Fig. 1,

$$\frac{\partial X_{T_f}}{\partial t_f} = V_{T_f}\cos\gamma_{T_f}, \qquad \frac{\partial Y_{T_f}}{\partial t_f} = V_{T_f}\sin\gamma_{T_f}$$

and

$$\omega_{T_f} \triangleq \frac{\partial \gamma_{T_f}}{\partial t_f}$$

Since the target trajectory is known, V_T, γ_T, and thus ω_T are known functions of time.

The constants λ_X and λ_Y are transformed to

$$\lambda_X = \lambda_r \cos\theta, \qquad \lambda_Y = \lambda_r \sin\theta \tag{23}$$

where $\lambda_r \triangleq \sqrt{(\lambda_X^2 + \lambda_Y^2)} \geq 0$ and $\theta \triangleq \tan^{-1}(\lambda_Y/\lambda_X)$. Using these definitions, Eq. (13) can be rewritten as

$$\dot{\lambda}_\gamma = -\lambda_r V_I \sin(\theta - \gamma_I) \tag{24}$$

and Eq. (22) becomes

$$\mathcal{H}_f = \lambda_r V_{T_f}\cos\left(\theta - \gamma_{T_f}\right) + \lambda_{\gamma_f}\omega_{T_f} \tag{25}$$

From Eq. (17), $\lambda_\chi = -1\ \forall t$, which is then used in Eq. (15) to obtain the optimal control input:

$$u^* = \frac{\lambda_\gamma}{V_I} \tag{26}$$

Substituting Eqs. (23) and (26) into Eq. (10), the Hamiltonian becomes

$$\mathcal{H} = \lambda_r V_I \cos(\theta - \gamma_I) + \frac{\lambda_\gamma^2}{2V_I^2} - k \tag{27}$$

Evaluating this equation at $t = t_f$, $\mathcal{H}_f$ is expressed as

$$\mathcal{H}_f = \lambda_r V_I \cos\left(\theta - \gamma_{I_f}\right) + \frac{\lambda_{\gamma_f}^2}{2V_I^2} - k \tag{28}$$

Equating Eqs. (25) and (28), λ_r is obtained:

$$\lambda_r = \frac{\lambda_{\gamma_f}^2/2V_I^2 - \lambda_{\gamma_f}\omega_{T_f} - k}{V_{T_f}\cos\left(\theta - \gamma_{T_f}\right) - V_I\cos\left(\theta - \gamma_{I_f}\right)} \tag{29}$$

If the denominator on the right-hand side equals zero, the numerator of this term provides a quadratic equation for λ_{γ_f}.

Since, as stated before, the Hamiltonian is constant along the optimal trajectory, equating Eqs. (27) and (28), λ_γ can be expressed as

$$\lambda_\gamma^2 = 2\lambda_r V_I^2\left[\cos\left(\theta - \gamma_{I_f}\right) - \cos(\theta - \gamma_I)\right] + \lambda_{\gamma_f}^2 \tag{30}$$

Using Eq. (30), the optimal control law given in Eq. (26) is expressed as

$$u^{*2} = 2\lambda_r V_I\left[\cos\left(\theta - \gamma_{I_f}\right) - \cos(\theta - \gamma_I)\right] + \frac{\lambda_{\gamma_f}^2}{V_I^2} \tag{31}$$

$$\operatorname{sign}(u^*) = \operatorname{sign}(\lambda_\gamma) \tag{32}$$

Thus, u^* depends on one time-varying variable only, the interceptor flight-path angle γ_I, and is defined by the unknown constants θ, λ_r, λ_{γ_f}, and γ_{I_f}. Here, λ_r, given in Eq. (29), depends on the unknown constants θ, λ_{γ_f}, γ_{I_f} and the target parameters at the final time (V_{T_f}, γ_{T_f}, and ω_{T_f}). Since the target trajectory is assumed to be known, the latter depend on t_f only. Thus, λ_r and the optimal control depend on the three constants θ, λ_{γ_f}, and γ_{I_f} and the interception time t_f. If these constants were known, the interceptor equations of motion (1–3) could be integrated. The formal solution of the interceptor trajectory, together with the interception boundary conditions in Eqs. (4–6) and an additional implicit relation for t_f will provide the necessary algebraic equations for these unknown parameters. In cases where λ_{γ_f} can be solved analytically, i.e., when the denominator on the right-hand side of Eq. (29) equals zero, the four unknowns of these equations will be θ, λ_r, γ_{I_f}, and t_f.

To integrate the equations of motion, the sign of the optimal control has to be determined. In general, any number of sign switches in the optimal control may exist along the extremal path. In practice, it is reasonable to assume that the optimal solution will be one of the following: 1) a single-turn maneuver obtained by a constant sign controller or 2) a two-turn maneuver, which involves one sign change in the control input, resulting in an S-shape trajectory. These two cases will be referred as NS (no switching) and S (switching), respectively. The optimal solution is selected by comparing the values of the performance indices in these two cases.

The equations will now be integrated for the two possible solutions.

A. NS-Maneuver Solution

The control function u^* does not vanish along an optimal trajectory, which also implies that

$$\dot{\gamma}_I \neq 0 \; \forall t \tag{33}$$

Substituting the optimal control of Eq. (31) into the dynamics of Eq. (3) yields

$$\dot{\gamma}_I^2 = 2\frac{\lambda_r}{V_I}\left[\cos\left(\theta - \gamma_{I_f}\right) - \cos(\theta - \gamma_I)\right] + \frac{\lambda_{\gamma_f}^2}{V_I^4} \tag{34}$$

It is interesting to note that when $\lambda_r = 0$, the optimal control is constant, leading to a constant rate of turn and a circular interception trajectory. This simple case is treated separately at the end of this section, and thus in the sequel it is assumed $\lambda_r > 0$.

Equation (34) is a first-order differential equation with only one dependent variable, the flight-path angle γ_I, and thus it can be solved by separation of variables. For that, the following state transformation is introduced:

$$\psi = \tfrac{1}{2}(\theta - \gamma_I) \tag{35}$$

with the boundary conditions on ψ

$$\psi(0) \triangleq \psi_0 = \tfrac{1}{2}\left(\theta - \gamma_{I_0}\right) \tag{36}$$

$$\psi(t_f) \triangleq \psi_f = \tfrac{1}{2}\left(\theta - \gamma_{I_f}\right) \tag{37}$$

With this state transformation and the assumption in Eq. (33), the differential equation (34), after some rearrangement, becomes

$$\mathrm{d}t = -\frac{C}{\sqrt{\left|\sin^2\psi - \left(\sin^2\psi_f - \lambda_{\gamma_f}^2/4\lambda_r V_I^3\right)\right|}}\,\mathrm{d}\psi \tag{38}$$

where

$$C \triangleq \operatorname{sign}(u^*)\sqrt{V_I/\lambda_r} \tag{39}$$

This equation can be directly integrated from $t = 0$ and $\psi = \psi_0$ to $t = t_f$ and $\psi = \psi_f$.[11] The integration results depend on the sign of the $\sin^2\psi_f - \lambda_{\gamma_f}^2/4\lambda_r V_I^3$ term in the denominator, leading to three possible solutions that correspond to the cases where this term is positive, zero, or negative. The integration results, presented in Appendix A, provide a relation between the final time t_f and the unknowns θ, λ_{γ_f}, and γ_{I_f}, involving elliptic integrals of the first kind, which formally can be stated as

$$t_f = \mathcal{T}\left(\theta, \lambda_{\gamma_f}, \gamma_{I_f}\right) \tag{40}$$

Since γ_{I_f} is a function of the interception time through the constraint equation (6), Eq. (40) is only implicit in t_f, and thus the latter cannot be evaluated explicitly using this equation.

Equations (1) and (2), after replacing ψ for γ_I and for the independent variable t by using Eqs. (35) and (38), respectively, are rearranged to yield

$$\mathrm{d}X_I = -\frac{CV_I\cos(\theta - 2\psi)}{\sqrt{\left|\sin^2\psi - \left(\sin^2\psi_f - \lambda_{\gamma_f}^2/4\lambda_r V_I^3\right)\right|}}\,\mathrm{d}\psi \tag{41}$$

$$\mathrm{d}Y_I = -\frac{CV_I\sin(\theta - 2\psi)}{\sqrt{\left|\sin^2\psi - \left(\sin^2\psi_f - \lambda_{\gamma_f}^2/4\lambda_r V_I^3\right)\right|}}\,\mathrm{d}\psi \tag{42}$$

The state variables X_I and Y_I can now be integrated from $X_I(0) = X_{I_0}$, $Y_I(0) = Y_{I_0}$, and $\psi = \psi_0$, up to their final values at t_f as stated in Eqs. (4) and (5), $X_I(t_f) = X_{T_f}$, $Y_I(t_f) = Y_{T_f}$, and $\psi = \psi_f$ to yield

$$X_{T_f} = X_{I_0} + V_I(A\cos\theta + B\sin\theta) \tag{43}$$

$$Y_{T_f} = Y_{I_0} + V_I(A\sin\theta - B\cos\theta) \tag{44}$$

where A and B can be evaluated in terms of elliptic integrals of the first and second kind and the constants θ, λ_{γ_f}, and γ_{I_f}, or formally,

$$A = \mathcal{A}\left(\theta, \lambda_{\gamma_f}, \gamma_{I_f}\right) \tag{45}$$

$$B = \mathcal{B}\left(\theta, \lambda_{\gamma_f}, \gamma_{I_f}\right) \tag{46}$$

A complete derivation of the above relations is presented in Appendix A.

The unknown parameters θ, λ_{γ_f}, γ_{I_f}, and t_f are obtained from a numerical solution of the four nonlinear algebraic equations: three boundary conditions in Eqs. (6), (43), and (44) and the interception time equation (40). With these parameters solved, the optimal control is obtained through Eq. (31) and its sign equals the sign of λ_{γ_f}.

For targets flying at constant flight-path angles, γ_{I_f} is given a priori by Eq. (6) and does not depend on the interception time. In these cases, t_f is explicit in θ and λ_{γ_f}, which are then determined by the two interception conditions.

B. S-Maneuver Solution

The sign of the optimal control input changes at some switching time t_s, i.e., it becomes zero at that time, $u^*(t_s) = 0$, and so does the adjoint variable λ_γ:

$$\lambda_\gamma(t_s) = 0 \tag{47}$$

With this assumption, Eq. (30) for λ_γ, evaluated at t_s, is rearranged to yield

$$\lambda_r = \frac{\lambda_{\gamma_f}^2}{2V_I^3\left[\cos\left(\theta - \gamma_{I_s}\right) - \cos\left(\theta - \gamma_{I_f}\right)\right]} \tag{48}$$

where γ_{I_s} denotes the interceptor flight-path angle at time t_s. Equating this equation to (29), a quadratic equation for λ_{γ_f} is obtained.

Using Eq. (48), the optimal control can be expressed as

$$u^{*2} = 2V_I\lambda_r\left[\cos\left(\theta - \gamma_{I_s}\right) - \cos(\theta - \gamma_I)\right] \tag{49}$$

and the equation for $\dot{\gamma}_I$ becomes

$$\dot{\gamma}_I^2 = 2\frac{\lambda_r}{V_I}\left[\cos(\theta - \gamma_{I_s}) - \cos(\theta - \gamma_I)\right] \tag{50}$$

To integrate Eq. (50), the state transformation of Eq. (35) is performed to yield

$$\mathrm{d}t = -\frac{C}{\sqrt{\left|\sin^2\psi - \sin^2\psi_s\right|}}\,\mathrm{d}\psi \tag{51}$$

where

$$\psi_s \triangleq \psi(t_s) = \tfrac{1}{2}(\theta - \gamma_{I_s}) \tag{52}$$

$$C \triangleq \mathrm{sign}(u^*)\sqrt{V_I/\lambda_r} \tag{53}$$

By assumption, the sign of u^* and therefore the sign of C change at t_s. Thus Eq. (51) is integrated in two parts: first, from $t = 0$ and $\psi = \psi_0$ to $t = t_s$ and $\psi = \psi_s$, and then from that time to $t = t_f$ and $\psi = \psi_f$. As in the NS case, the integration results (presented in Appendix B) provide an implicit relation between t_f and the three unknowns θ, γ_{I_s}, and γ_{I_f}. The first part of the integral (from ψ_0 to ψ_s) is the switching time t_s expressed in terms of these constants.

Now the transformation equation (35) together with Eq. (51) is used to rearrange the dynamics equations (1) and (2):

$$\mathrm{d}X_I = -\frac{CV_I\cos(\theta - 2\psi)}{\sqrt{\left|\sin^2\psi - \sin^2\psi_s\right|}}\,\mathrm{d}\psi \tag{54}$$

$$\mathrm{d}Y_I = -\frac{CV_I\sin(\theta - 2\psi)}{\sqrt{\left|\sin^2\psi - \sin^2\psi_s\right|}}\,\mathrm{d}\psi \tag{55}$$

which also are integrated in two parts. The integration results, presented in Appendix B, are used in the interception boundary conditions of Eqs. (4) and (5), as before. The resulting two nonlinear algebraic equations together with the implicit equation for t_f provide three implicit algebraic equations for the three unknowns θ, γ_{I_s}, and γ_{I_f} (or t_f), and they have to be solved numerically, similar to the NS solution. These parameters determine the time history of the optimal control input through Eq. (49).

The sign of the optimal control equals the sign of λ_γ, which is obtained from Eq. (24), repeated here for convenience:

$$\dot{\lambda}_\gamma = -\lambda_r V_I \sin(\theta - \gamma_I)$$

Since, by assumption, $\lambda_\gamma(t_s) = 0$, the sign of λ_γ for $t < t_s$ is opposite to the sign of the derivative $\dot{\lambda}_\gamma$ at t_s. Thus, since, by definition, $\lambda_r \geq 0$, the sign of the optimal control u^* for that time interval is given by

$$\mathrm{sign}[u^*(t)] = \mathrm{sign}\left[\sin(\theta - \gamma_{I_s})\right] \qquad \text{for} \qquad t < t_s \tag{56}$$

and is opposite in sign for $t > t_s$. Note that this equation does not add additional unknowns and depends on the same parameters θ and γ_{I_0}.

IV. Special Cases

Two special cases of planar interception are discussed in this section: a case for which the final flight-path angle is free and a case for which the initial flight-path angle is optimally chosen. These two problems can be easily solved using the results of the previous section.

A. Free γ_{I_f}

This problem was solved in Ref. 8 for a maneuvering target and in Ref. 9 for a nonmaneuvering target. In both cases relative coordinates were employed.

The results obtained in this work, expressed in absolute coordinates, can be easily reduced to the solutions obtained in Refs. 8 and 9. Since γ_{I_f} is free, the transversality condition implies that $\lambda_{\gamma_f} = 0$. Using this boundary condition in Eqs. (29–31), the optimal control is expressed as

$$u^{*2} = \frac{2kV_I}{V_{T_f}\cos(\theta - \gamma_{T_f}) - V_I\cos(\theta - \gamma_{I_f})} \times \left[\cos(\theta - \gamma_I) - \cos(\theta - \gamma_{I_f})\right] \tag{57}$$

which is identical to the result in Ref. 8. Algebraic manipulation shows that the same result was obtained in Ref. 9.

B. Optimal γ_{I_0}

In this problem the initial flight-path angle γ_{I_0} is not known, whereas γ_{I_f} is specified as before in Eq. (6).

Since the initial value of γ_I is not specified and has to be chosen optimally, the initial value of λ_γ is

$$\lambda_\gamma(0) = 0 \tag{58}$$

Using this boundary condition and evaluating Eq. (30) at $t = 0$ yields

$$\lambda_r = \frac{\lambda_{\gamma_f}^2}{2V_I^3\left[\cos(\theta - \gamma_{I_0}) - \cos(\theta - \gamma_{I_f})\right]} \tag{59}$$

As in the S case of the previous section, equating this result to Eq. (29) provides a quadratic equation for λ_{γ_f}, where the unknown constants are θ, γ_{I_0}, γ_{I_f}, and t_f. In this case the optimal control is given by

$$u^{*2} = 2\lambda_r V_I\left[\cos(\theta - \gamma_{I_0}) - \cos(\theta - \gamma_I)\right] \tag{60}$$

and the optimal trajectory equations can be integrated using the same state transformation of Eq. (35). The integration results are presented in Appendix C and provide four implicit nonlinear algebraic equations for the unknowns θ, γ_{I_0}, γ_{I_f}, and t_f.

To perform this integration, it is assumed that the optimal solution involves a turn in one direction only, i.e., $\dot{\gamma}_I$ and thus $u^* \neq 0$ except at the initial time. The sign of the optimal control is determined by the sign of λ_γ, Eq. (32), and is obtained from Eq. (24). From the initial condition $\lambda_\gamma(0) = 0$ it is concluded that the sign of λ_γ and thus the sign of the optimal control u^* equal the sign of $\dot{\lambda}_\gamma$ at the initial time and can be obtained by evaluating the above equation at $t = 0$:

$$\mathrm{sign}(u^*) = -\mathrm{sign}\left[\sin(\theta - \gamma_{I_0})\right] \tag{61}$$

For the case where both the initial and final flight-path angles are free and energy only is minimized ($k = 0$), from Eq. (29), $\lambda_r = 0$ and consequently the optimal trajectory is a straight line.

V. Examples

Interception trajectories obtained using the optimal control law derived in the previous sections are presented here. In the first two examples, the target is moving along a circular path at a constant velocity and a constant rate of turn $\dot{\gamma}_T = 4$ deg/s. The interceptor–target velocity ratio was set to $V_I/V_T = 1.25$. The interceptor is fired from the origin of the reference system along the y axis and a head-on interception is required, i.e., $\gamma_{I_0} = 90$ deg and $\Gamma_f = 180$ deg. Two different values of the weight factor k in the performance index J Eq. (7) are examined: $k = 8000$ and $k = 3500$. The former expresses a case for which a larger emphasis on the interception time is specified relative to the latter. In addition, the optimal γ_{I_0} interception problem is solved for each k.

The interceptor and target trajectories for the $k = 8000$ example are presented in Fig. 2, showing the NS and S solutions and the solution for optimal γ_{I_0}, which in this case is obtained for $\gamma_{I_0} = -8.3$ deg. The head-on interception requirement is met by all the solutions. The interceptor–target acceleration ratios as a function of time are given in Fig. 3, showing that the control input of the S solution changes sign at $t = 21.4$ s. The performance indices are normalized by the value of J for the optimal γ_{I_0} case, J_{opt}. In this example the performance index of the S solution is lower than that of the NS solution and thus the S maneuver is chosen as the optimal solution. In these figures it can be seen that the interception time,

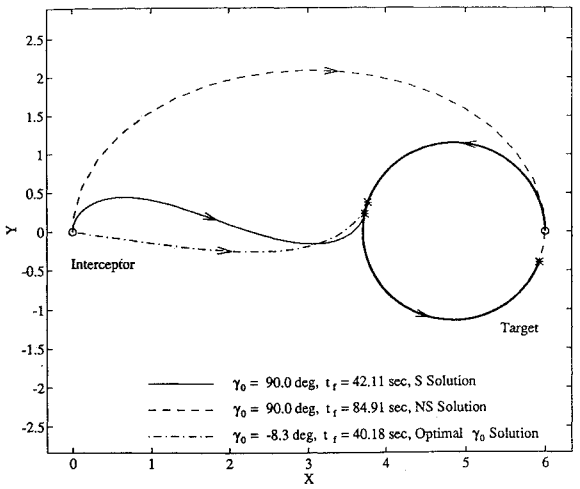

Fig. 2 Example 1: Trajectories of head-on interception with $\gamma_{I_0} = 90$ deg and optimal $\gamma_{I_0} = -8.3$ deg. ○, ∗: Launch and intercept points, respectively.

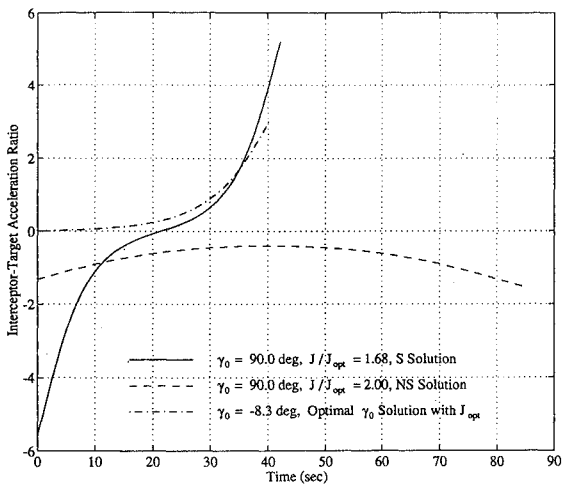

Fig. 3 Example 1: Interceptor-target acceleration ratio for head-on interception with $\gamma_{I_0} = 90$ deg and optimal $\gamma_{I_0} = -8.3$ deg for $k = 8000$.

the maximum control input, and of course the performance index of the solution with optimal γ_{I_0} are lower compared to the case with specified $\gamma_{I_0} = 90$ deg.

In the second example the emphasis on t_f in the performance measure is reduced by setting $k = 3500$. The trajectories and the acceleration ratios are very similar to those of the first example. However, the performance index is different, due to the different penalty on the interception duration. The cost ratio for the NS case is $J/J_{\text{opt}} = 1.84$ and for the S case $J/J_{\text{opt}} = 2.25$, where J_{opt} is the performance measure of the optimal $\gamma_{I_0} = -10.9$ deg solution. Hence, the optimal solution for this example is the NS maneuver. It should be noted that, in practice, the nominal value of the cost function is of less importance, and the selection of the preferred solution should be based on the nature of the results.

In an additional example, head-on optimal interception of a ballistic missile in the boost phase is computed. In computing the target trajectory, constant thrust and constant turn rate are assumed. The missile is launched vertically while the interceptor is fired horizontally. The interception trajectory obtained using the optimal control law, which resulted in an S-type maneuver, is presented in Fig. 4. Also shown is the trajectory obtained for an interceptor fired at an optimal $\gamma_{I_0} = 43.4$ deg. Although the intercept time of the latter is longer, the performance index obtained for this case is smaller by 13% compared to the performance index for the $\gamma_{I_0} = 0$ deg case.

It should be pointed out that the required head-on interception could not be obtained using guidance laws such as pure proportional navigation, and thus the optimal solutions presented in this work should be used when the interception geometry is prescribed.

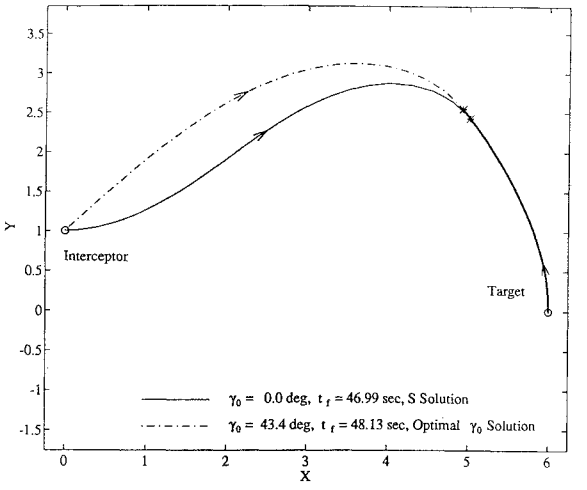

Fig. 4 Example 3: Trajectories of head-on interception of a ballistic target at boost with $\gamma_{I_0} = 0$ deg and optimal $\gamma_{I_0} = 43.4$ deg. ○, ∗: Launch and interception points, respectively.

VI. Conclusions

In this paper, interception laws for maneuvering targets with predetermined trajectories were presented. The interception problem included a requirement on the interception geometry, thus imposing terminal boundary conditions on the interceptor flight-path angle. Analytical solutions of this problem were derived, where the optimal control law is expressed as an explicit function of the current value of the flight-path angle and depends on four parameters: three constants and the optimal interception time. These parameters are obtained by numerically solving four nonlinear algebraic equations, derived from an analytical solution of the equations of motion, while satisfying the necessary conditions and the terminal constraints. Multiple solutions exist, which depend on the number of sign changes in the control function during the intercept. The optimal solution is the one that renders the smallest cost. In practice, it is reasonable to assume that the control will switch sign no more than once along the trajectory. With this assumption, optimal trajectories were computed for several representative examples with head-on interception requirements. Solutions with optimal initial conditions and thus superior performance were presented for cases where the interceptor initial flight-path angle can be freely assigned.

Appendix A: Analytic Solution for NS Maneuver

The NS maneuver is characterized by a control input that does not become zero along the optimal solution. The three differential equations that describe this solution are

$$dt = -\frac{C}{\sqrt{\left|\sin^2\psi - \left(\sin^2\psi_f - \lambda_{\gamma_f}^2/4\lambda_r V_I^3\right)\right|}}\,d\psi \tag{A1}$$

$$dX_I = -\frac{CV_I\cos(\theta - 2\psi)}{\sqrt{\left|\sin^2\psi - \left(\sin^2\psi_f - \lambda_{\gamma_f}^2/4\lambda_r V_I^3\right)\right|}}\,d\psi \tag{A2}$$

$$dY_I = -\frac{CV_I\sin(\theta - 2\psi)}{\sqrt{\left|\sin^2\psi - \left(\sin^2\psi_f - \lambda_{\gamma_f}^2/4\lambda_r V_I^3\right)\right|}}\,d\psi \tag{A3}$$

where

$$C \triangleq \text{sign}(u^*)\sqrt{V_I/\lambda_r} \tag{A4}$$

and ψ was defined in Eqs. (35–37). The limits of integration are

$$\begin{aligned} t = 0 &\Rightarrow t = t_f \\ \psi(0) = \psi_0 &\Rightarrow \psi(t_f) = \psi_f \\ X_I(0) = X_{I_0} &\Rightarrow X_I(t_f) = X_{I_f} \\ Y_I(0) = Y_{I_0} &\Rightarrow Y_I(t_f) = Y_{I_f} \end{aligned} \tag{A5}$$

The analytical integration results in explicit nonlinear relations between t_f, X_{I_f}, and Y_{I_f} and parameters describing the optimal interception solution, i.e., θ, $\lambda_{\gamma_f}^2$, and γ_{I_f}. The solutions for X_{I_f} and Y_{I_f} have the form given in Eqs. (43) and (44).

The integration results depend on the sign of the $\sin^2\psi_f - \lambda_{\gamma_f}^2/4\lambda_r V_I^3$ term in the denominator, leading to three possible solutions denoted by NS_+, NS_0, and NS_-. In addition there is a constant rate-of-turn solution, denoted by NS_c below.

Case NS_+: $\sin^2\psi_f > \lambda_{\gamma_f}^2/(4\lambda_r V_I^3)$. From Eq. (31), the condition for positive u^{*2} is

$$\min\left(\sin^2\psi_0, \sin^2\psi_f\right) > \sin^2\psi_f - \frac{\lambda_{\gamma_f}^2}{4\lambda_r V_I^3} \triangleq d_+^2 \tag{A6}$$

The integration results are[11]

$$t_{f_+} = C[F(\alpha_{f_+}, m_+) - F(\alpha_{0_+}, m_+)] \tag{A7}$$

$$A_+ = t_{f_+} - 2C[E(\alpha_{f_+}, m_+) - E(\alpha_{0_+}, m_+)] \tag{A8}$$

$$B_+ = 2C\left[\sqrt{\sin^2\psi_0 - d_+^2} - \sqrt{\sin^2\psi_f - d_+^2}\right] \tag{A9}$$

where

$$m_+ = \sqrt{1 - d_+^2} \tag{A10}$$

$$\alpha_{0_+} = \sin^{-1}\frac{\cos\psi_0}{m_+} \tag{A11}$$

$$\alpha_{f_+} = \sin^{-1}\frac{\cos\psi_f}{m_+} \tag{A12}$$

Here, F is the elliptic and K is the complete elliptic integral of first kind; E is the elliptic and $\boldsymbol{E}$ is the complete elliptic integral of the second kind.

Case NS_0: $\sin^2\psi_f = \lambda_{\gamma_f}^2/(4\lambda_r V_I^3)$. In this case the solution is[11]

$$t_{f_0} = C\ell n\left[\frac{\tan(\psi_0/2)}{\tan(\psi_f/2)}\right] \tag{A13}$$

$$A_0 = t_{f_0} + 2C(\cos\psi_0 - \cos\psi_f) \tag{A14}$$

$$B_0 = 2C(\sin\psi_0 - \sin\psi_f) \tag{A15}$$

Case NS_-: $\sin^2\psi_f < \lambda_{\gamma_f}^2/(4\lambda_r V_I^3)$. Define

$$d_-^2 \triangleq \frac{\lambda_{\gamma_f}^2}{4\lambda_r V_I^3} - \sin^2\psi_f > 0 \tag{A16}$$

to obtain the solution[11]

$$t_{f_-} = Cm_-[F(\alpha_{0_-}, m_-) - F(\alpha_{f_-}, m_-)] \tag{A17}$$

$$A_- = (1 + 2d_-^2)t_{f_-} + C\left\{\frac{2}{m_-}[E(\alpha_{f_-}, m_-) - E(\alpha_{0_-}, m_-)] + \frac{\sin(2\psi_0)}{\sqrt{\sin^2\psi_0 + d_-^2}} - \frac{\sin(2\psi_f)}{\sqrt{\sin^2\psi_f + d_-^2}}\right\} \tag{A18}$$

$$B_- = 2C\left[\sqrt{\sin^2\psi_0 + d_-^2} - \sqrt{\sin^2\psi_f + d_-^2}\right] \tag{A19}$$

where

$$m_- = \frac{1}{\sqrt{1 + d_-^2}} \tag{A20}$$

$$\alpha_{0_-} = \sin^{-1}\frac{\sin\psi_0/m_-}{\sqrt{\sin^2\psi_0 + d_-^2}} \tag{A21}$$

$$\alpha_{f_-} = \sin^{-1}\frac{\sin\psi_f/m_-}{\sqrt{\sin^2\psi_f + d_-^2}} \tag{A22}$$

Case NS_c: $\lambda_r = 0$. In this case the optimal control is constant:

$$u^* = \sqrt{\lambda_{\gamma_f}/V_I} \tag{A23}$$

and thus the equations of motion (1–3) can be easily integrated to obtain

$$t_{f_c} = C\left(\gamma_{I_f} - \gamma_{I_0}\right) \tag{A24}$$

$$X_{I_f} = X_{I_0} + CV_I\left(\sin\gamma_{I_f} - \sin\gamma_{I_0}\right) \tag{A25}$$

$$Y_{I_f} = Y_{I_0} + CV_I\left(\cos\gamma_{I_0} - \cos\gamma_{I_f}\right) \tag{A26}$$

where

$$C \triangleq \text{sign}(u^*)\frac{V_I^2}{\lambda_{\gamma_f}} \tag{A27}$$

Appendix B: Analytic Solution for S Maneuver

In the S-maneuver solution the optimal control input is changing its sign at the switching time t_s. The three equations that are integrated to obtain the solution are

$$\mathrm{d}t = -\frac{C}{\sqrt{\left|\sin^2\psi - \sin^2\psi_s\right|}}\,\mathrm{d}\psi \tag{B1}$$

$$\mathrm{d}X_I = -\frac{CV_I\cos(\theta - 2\psi)}{\sqrt{\left|\sin^2\psi - \sin^2\psi_s\right|}}\,\mathrm{d}\psi \tag{B2}$$

$$\mathrm{d}Y_I = -\frac{CV_I\sin(\theta - 2\psi)}{\sqrt{\left|\sin^2\psi - \sin^2\psi_s\right|}}\,\mathrm{d}\psi \tag{B3}$$

where

$$C \triangleq \text{sign}(u^*)\sqrt{V_I/\lambda_r} \tag{B4}$$

The sign on the right-hand side of these equations changes at t_s, and thus the integration is performed in two parts: first integrate from $t = 0$ and $\psi = \psi_0$ to $t = t_s$ and $\psi = \psi_s$, where the optimal control and thus λ_γ become zero. The final time of this part is the switching time t_s of the S maneuver. Then integrate the equations with an opposite sign from $t = t_s$ and $\psi = \psi_s$ to $t = t_f$ and $\psi = \psi_f$. Again, the interception location (X_{I_f}, Y_{I_f}) has the form given in Eqs. (43) and (44).

The condition for positive u^{*2} is [see Eq. (49)]

$$\min\left(\sin^2\psi_0, \sin^2\psi_f\right) > \sin^2\psi_s \tag{B5}$$

and the integration results are[11]

$$t_s = C[K(\cos\psi_s) - F(\alpha_0, \cos\psi_s)] \tag{B6}$$

$$t_f = C[2K(\cos\psi_s) - F(\alpha_0, \cos\psi_s) - F(\alpha_f, \cos\psi_s)] \tag{B7}$$

$$A = t_f - 2C[2\boldsymbol{E}(\cos\psi_s) - E(\alpha_0, \cos\psi_s) - E(\alpha_f, \cos\psi_s)] \tag{B8}$$

$$B = 2C\left[\sqrt{\sin^2\psi_0 - \sin^2\psi_s} + \sqrt{\sin^2\psi_f - \sin^2\psi_s}\right] \tag{B9}$$

where

$$\alpha_0 = \sin^{-1}\frac{\cos\psi_0}{\cos\psi_s} \tag{B10}$$

$$\alpha_f = \sin^{-1}\frac{\cos\psi_f}{\cos\psi_s} \tag{B11}$$

Appendix C: Analytic Solution—Optimal γ_{I_0}

To obtain the analytic solution to the interception with optimal initial flight-path angle γ_{I_0}, three differential equations are integrated:

$$dt = -\frac{C}{\sqrt{|\sin^2\psi - \sin^2\psi_0|}}\,d\psi \tag{C1}$$

$$dX_I = -\frac{CV_I\cos(\theta - 2\psi)}{\sqrt{|\sin^2\psi - \sin^2\psi_0|}}\,d\psi \tag{C2}$$

$$dY_I = -\frac{CV_I\sin(\theta - 2\psi)}{\sqrt{|\sin^2\psi - \sin^2\psi_0|}}\,d\psi \tag{C3}$$

where

$$C \triangleq \text{sign}(u^*)\sqrt{V_I/\lambda_r} \tag{C4}$$

The limits of integration are similar to those specified in Eqs. (A5) and X_{I_f} and Y_{I_f} are expressed as in Eqs. (43) and (44), respectively.

The condition to ensure positive u^{*2} in Eq. (60) is

$$\sin^2\psi_f > \sin^2\psi_0 \tag{C5}$$

and the solution is given by[11]

$$t_f = C[F(\alpha_f, \cos\psi_0) - K(\cos\psi_0)] \tag{C6}$$

$$A = t_f - 2C[E(\alpha_f, \cos\psi_0) - \boldsymbol{E}(\cos\psi_0)] \tag{C7}$$

$$B = -2C\sqrt{\sin^2\psi_f - \sin^2\psi_0} \tag{C8}$$

where

$$\alpha_f = \sin^{-1}\frac{\cos\psi_f}{\cos\psi_0} \tag{C9}$$

Acknowledgment

This research was supported by the fund for the promotion of research at the Technion.

References

[1]Kreindler, E., "Optimality of Proportional Navigation," *AIAA Journal*, Vol. 11, No. 6, 1973, pp. 878–880.

[2]Bryson, A. E., Jr., and Ho, Y., *Applied Optimal Control*, Hemisphere, Washington, DC, 1975.

[3]Nesline, F. W., and Zarchan, P., "A New Look at Classical versus Modern Homing Missile Guidance," *Journal of Guidance, Control, and Dynamics*, Vol. 4, No. 1, 1981, pp. 78–85.

[4]Cottrell, R. G., "Optimal Intercept Guidance for Short-Range Tactical Missiles," *AIAA Journal*, Vol. 9, No. 7, 1971, pp. 1414–1415.

[5]Sridhar, B., and Gupta, N. K., "Missile Guidance Laws Based on Singular Perturbation Methodology," *Journal of Guidance, Control, and Dynamics*, Vol. 3, No. 2, 1980, pp. 158–165.

[6]Shinar, J., "Validation of Zero Order Feedback Strategies for Medium Range Air-to-Air Interception in a Horizontal Plane," NASA TM 84237, April 1982.

[7]Menon, P. K. A., and Briggs, M. M., "Near Optimal Midcourse Guidance for Air-to-Air Missiles," *Journal of Guidance, Control, and Dynamics*, Vol. 13, No. 4, 1990, pp. 596–602.

[8]Guelman, M., and Shinar, J., "Optimal Guidance Law in the Plane," *Journal of Guidance, Control, and Dynamics*, Vol. 7, No. 4, 1984, pp. 471–476.

[9]Hull, D. G., Radke, J. J., and Mack, R. E., "Time-to-Go Prediction for Homing Missiles Based on Minimum-Time Intercepts," *Journal of Guidance, Control, and Dynamics*, Vol. 14, No. 5, 1991, pp. 865–871.

[10]Glizer, V. Y., "Optimal Planar Interception with Fixed End Conditions," *Journal of Optimization Theory and Applications* (to be published).

[11]Gradshtein, I. S., and Ryzhik, I. M., *Table of Integrals, Series and Products*, Academic, New York, 1980.